GEOMETRIC OPTIMIZATION OF AN OVERTOPPING WAVE ENERGY CONVERTER FOR DEEP WATER FLOW

Bianca Neves Machado, biancanevesmachado@gmail.com
Mateus das Neves Gomes, mateusufpel.gomes@gmail.com
Universidade Federal do Rio Grande do Sul, Rua Sarmento Leite, 425, CP. 90050-170, Porto Alegre, RS, Brasil

Jeferson Avila Souza, jasouza@furg.br
Paulo Roberto de Freitas Teixeira, pauloteixeira@furg.br
Liércio André Isoldi, liercioisoldi@furg.br
Universidade Federal do Rio Grande, Rua Sarmento Leite 425, CP. 474, Rio Grande, RS, Brasil

Luiz Alberto Oliveira Rocha, luizrocha@mecanica.ufrgs.br
Universidade Federal do Rio Grande do Sul, Rua Sarmento Leite, 425, CP. 90050-170, Porto Alegre, RS, Brasil

Elizaldo Domingues dos Santos, elizaldosantos@furg.br
Universidade Federal do Rio Grande, Avenida Itália km. 8, CP. 474, Rio Grande, RS, Brasil

Abstract. *Nowadays it is estimated that ocean wave energy has a potential of nearly 10 TW, from this energy 10 % to 25 % can be converted into electrical one. As a consequence, there are several technologies being developed, an example is the overtopping converter. The device operational principle consists of a ramp which guides incoming waves into a reservoir raised slightly above sea level. The potential energy of the water trapped in the reservoir is then converted to electrical energy through a low head turbine connected to a generator. In this sense, the present work shows a numerical study concerned with the geometric optimization of an overtopping wave energy converter (WEC) for a deep water monochromatic wave (relative depth of $h/\lambda = 0.62$). The main purpose here is the achievement of a theoretical recommendation by means of Constructal Design for the ramp geometry (ratio between the ramp height and length: H_1/L_1) which increases the amount of water that insides the reservoir. Other goal is the comparison of the optimal geometry obtained here for $h/\lambda = 0.62$ with previous results of literature for $h/\lambda = 0.5$. In the present simulations, it is considered a two-dimensional laboratory scale wave tank with an overtopping device placed inside. The computational domain was generated in software GAMBIT and the governing equations (conservation equations of mass, momentum and an equation for the transport of volumetric fraction) were solved with a Computational Fluid Dynamics (CFD) package based on the finite volume method (MVF), FLUENT®. Concerning the wave generation, it was imposed velocity boundary conditions in the inlet of the wave tank using User Defined Functions (UDF) to mimics the effect of a wavemaker. To tackle with the mixture water-air it was used the multiphase model Volume of Fluid (VOF). For the relative depth of $h/\lambda = 0.62$, the results show a dependence of the mass of water that insides de reservoir as a function of the ramp geometry (ratio H_1/L_1), which is in agreement with the previous studies of literature for other relative depth of $h/\lambda = 0.5$. However, there is no universal shape that leads to the best performance for several wave climates. For example, for $h/\lambda = 0.5$ the optimal shape for the ramp was achieved for $(H_1/L_1)_o = 0.6$, while for $h/\lambda = 0.5$ this value was $(H_1/L_1)_o = 0.4$.*

Keywords: *Constructal design, geometric optimization, overtopping WEC, numerical study*

1. NOMENCLATURE

h	Depth, m
H	Wave height, m
H_1	Height of the ramp, m
H_T	Height of the wave tank, m
L_1	Length of the ramp, m
L_T	Length of the wave tank, m
$\dot{m}$	Mass flow rate, $kg \cdot s^{-1}$
T	Period of the wave, s
t	Temporal domain, s

Greek symbols

ϕ	Device volume fraction
λ	Wave length, m

Subscripts

m	Maximum amount of mass that enters into the reservoir
o	Optimal

2. INTRODUCTION

The augmentation of energy demand and the Kyoto agreement to reduce the greenhouse gas emissions have increased the interest for the study of renewable energy (Beels et al., 2010). Other benefits of the employment of these kind of energy can be mentioned, e.g., minimization of the fossil fuel deposits exploration and its environmental

associated impacts (Tolmasquim, 2003). These aspects unveil the need for the development of scientific and technological studies about the devices of wave energy converters, allowing a large scale energy supply.

The ocean can be considered as an inexhaustible source of alternative and renewable energy which is found in the waves (that are generated by the action of the winds over the ocean surface), in the maritime currents (caused by the tidal effects and by the changes in salinity and temperature of the water). Nowadays, this fact is even more relevant due to crescent need for the obtainment of sustainable energy sources associated with the decrease of conventional energy sources (Lima, 2010).

In Fig. 1 it is possible to observe that the wave energy is distributed over the Earth in am unequal way. Accordingly Lima (2010), the best wave energy regions must have a minimal power level between 20 and 70kW/m. Brazil has a coastline where the power level is around 30kW/m, justifying the development of researches in this subject.

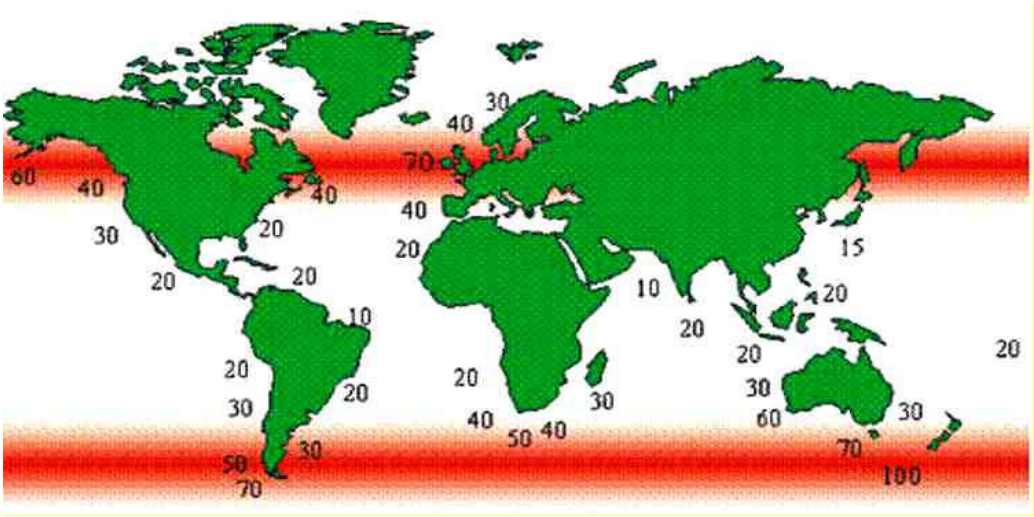

Figure 1. Global wave power distribution, in kW/m of crest length.
(CENTER FOR RENEWABLE ENERGY SOURCES, 2002)

In this context, the conversion of the ocean wave energy into electrical energy has been studied in the last years. In accordance with Ribeiro (2007) this kind of energy is 10 to 30 times more concentrated which solar energy, per area of incidence. There are several proposed technologies for transformation of the wave energy into electricity, however any of them yet consolidated.

The devices for conversion of wave energy into electrical one can be classified according to its main operational principle in three main classes (Cruz and Sarmento, 2004):

- oscillating water column – OWC;
- body oscillating – point absorbers or surging devices;
- overtopping devices.

The overtopping device, which is the scope of the present work, Fig. 2, consists of a ramp that captures the water that is close to the wave crest and introduces it, by over spilling, into a reservoir where it is stored at a level higher than the average free-surface level of the surrounding sea. The potential energy of water trapped in the reservoir is then converted to electrical energy through a low head turbine connected to a generator (WAVEC, 2004).

It is worthy to mention that, some tests with prototypes are presented into the literature, e.g. Wave Dragon, Wave Plane and Seawave Slot-Cone Generator (Falcão, 2010). Concerning the numerical evaluation of overtopping device, Beels et al. (2010) employed time-dependent mild-slope equations to model single and multiple Wave Dragon WECs, Neves et al. (2010) compared three numerical methods for estimative of the mean volume that overcomes the ramp: Amazonia (based on the solution of non-linear equations for shallow waves), Cobras-UC (an eulerian model which uses VOF for the multiphase flow) and SPHysics, Iahnke (2010) evaluated the ramp inclination of an overtopping device for a two dimensional flow and Machado et al. (2011) evaluated the geometrical optimization of an overtopping energy converter by means of Constructal Design (Bejan and Lorente, 2008) for a relative depth of $h/\lambda = 0.5$. The basic idea of the latter work is dissimilar from that performed by Iahnke (2010), which evaluate geometries without comply with the device volume constraint.

The present work aims to discover, by means of the Constructal method, the geometrical optimization of the main operational principle of an overtopping energy converter for a relative depth of $h/\lambda = 0.5$. The main purpose is to evaluate the influence of the relative depth over the optimal geometry of the ramp (H_1/L_1) which leads to the highest amount of water that enters into the converter reservoir.

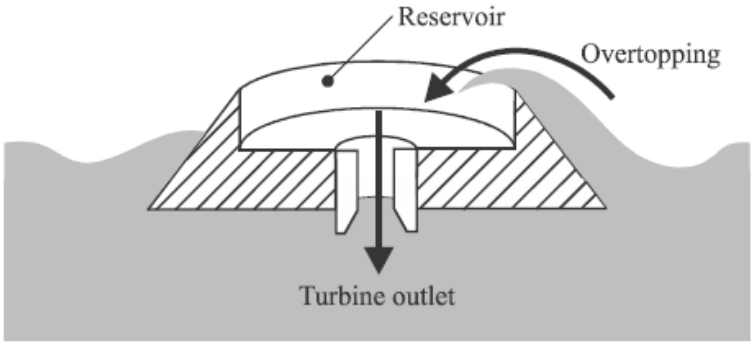

Figure 2. Illustration of the main operational principle of the overtopping device.

Constructal Design, which is employed here for determination of optimal geometry of overtopping device, has been used to explain deterministically the shape generation of flux structures in nature such as: rivers basin, lungs, flows in atmosphere, animal shapes, vascular tissues and others, according to an evolutionary principle of flow access in time. This principle is the Constructal law, which states that "for a flow system to persist in time (to survive), it must evolve in such way that it provides easier and easier access to the currents that flow through it" (Bejan and Lorente, 2008). This same principle is also used for design of shapes in several areas as cooling of packages, fuel cells, fins, heat exchangers and others (Bejan and Lorente, 2006). The employability of the law for flux systems in engineering has been called Constructal Design.

3. METHODOLOGY

The analyzed physical problem consists of a two dimensional overtopping device placed in a wave tank, as depicted in Fig. 3. The third dimension W is perpendicular to the plane of the figure. The wave flow is generated by an imposition of a velocity field in the left surface of the tank. The generated waves reach the ramp and the crest water can be spilled into the reservoir.

In the constructal design framework, the optimization of the present problem is subjected to two constraints, namely, the total area of the wave tank constraint ($A = H_T \cdot L_T$) and the area of the ramp constraint ($A_r = H_1 \cdot L_1/2$) and varying the geometry degrees of freedom to achieves one objective, which in this case is the maximization of the mass of water that enters into the reservoir of the overtopping device. The dimensionless form of the ramp area is given by the ratio between the ramp and wave tank areas (ϕ). The objective of the analysis is to determine the optimal geometry (H/λ, h/λ, H/h and H_1/L_1) that leads to the maximum mass flow rate of water entering in the reservoir. As previously mentioned, the degree of freedom H_1/L_1 is optimized, keeping fixed the other parameters: $\phi = 0.02$, $H/\lambda = 0.14$ (the ratio between the wave height and its length, also known as wave slope), $h/\lambda = 0.62$ (relative depth) and $H/h = 0.23$ (the ratio between the wave height and the depth, relative wave height). Moreover, the following dimensions and parameters are assumed: $H_T = 1.0$ m, $L_T = 8.0$ m, $L_2 = 0.5$ m, $L_3 = 3.0$ m, $H = 0.14$ m, $\lambda = 0.97$ m, $h = 0.6$ m and $T = 0.8$ s.

For the treatment of this kind of flow, the VOF formulation, which is based on the hypothesis of two or more impenetrable phases, is employed. Since the ratio of the density between water and air on the mixture is much higher than unity, it is expected that this treatment leads to excellent predictions of the phenomenon. It is worth to mention that for each control volume, the sum of the volumetric fractions for all involved phases is unity.

The variable and property fields are shared by the phases and represent averaged values on the volume. It is necessary to know each volumetric fraction of the mixture. The variables and properties for a specific volume represent one of the phases or a mixture of phases, depending on the values of the volume fraction. For a qth volumetric fraction of the fluid, named α_q, three configurations are presented (Liu et al., 2008a, Liu et al., 2008b):

$\alpha_q = 0$: the volume is empty (for a q_0 fluid);

$\alpha_q = 1$: the volume is full (for a q_0 fluid);

$0 < \alpha_q < 1$: the volume of q_0 fluid has interface with other phases;

For each volume domain, the properties are obtained as a function of the local value of α_q. The placement among the phases is defined from the mass equation solution for the fraction of one or more phases. For the phase q_0, the continuity equation is given by:

$$\frac{\partial}{\partial t}\left(\alpha_q \rho_q\right) + \nabla\left(\alpha_q \rho_q \vec{v}_q\right) = S_{\alpha_q} + \sum_{p=1}^{n}\left(\dot{m}_{pq} - \dot{m}_{qp}\right) \tag{1}$$

where $\dot{m}_{qp}$ is the rate of mass transfer from phase q to phase p (kg·m^{-3}·s^{-1}), $\dot{m}_{pq}$ is the rate of mass transfer from phase p to phase q (kg·m^{-3}·s^{-1}) and $S_{\alpha q}$ is the mass source term, which is null in the present study. The volume fraction equation is not solved for the primary phase, being computed based on the following restriction:

$$\sum_{q=1}^{n} \alpha_q = 1 \tag{2}$$

For a system with n phases, the density is obtained from the weighting of the related phases. Therefore, density can be written by:

$$\rho = \sum \alpha_q \rho_q \tag{3}$$

The momentum equations are solved for the mixture water-air and the velocity fields are shared among the phases. The momentum equations can be written in its vetorial notation by:

$$\frac{\partial}{\partial t}(\rho \vec{v}) + \nabla(\rho \vec{v}\vec{v}) = -\nabla p + \nabla\left(\bar{\bar{\tau}}\right) + \rho\vec{g} + \vec{F} \tag{4}$$

where p is the static pressure (N·m^{-2}), $\bar{\bar{\tau}}$ is the viscous stress tensor (N·m^{-2}), $\vec{g}$ is the gravitational acceleration (m·s^{-2}) and $\vec{F}$ represents external body forces (N·m^{-3}).

In order to obtain the volumetric fraction of one phase, an additional equation is solved for the volumetric fraction, which is written by:

$$\frac{\partial}{\partial t}(\rho \alpha_q) + \nabla(\rho \vec{v} \alpha_q) = 0 \tag{5}$$

For the waves generation, it is employed a user defined function (UDF) for the entrance velocity of the channel, simulating the wavemaker behavior, in this evaluation the inlet velocity varies in space and time according to the Stokes Theory of 2nd order. This method is the same one employed in the previous study of Gomes et al. (2009). The velocities in x and z directions for the entrance channel are, respectively, given by:

$$u = Agk\frac{\cosh(kz+kh)}{\omega\cosh(kh)}\cos(kx-\omega t) + \frac{3}{4}A^2\omega k\frac{\cosh 2k(k+z)}{senh^4(kh)}\cos 2(kx-\omega t) \tag{6}$$

$$w = Agk\frac{senh(kz+kh)}{\omega\cosh(kh)}sen(kx-\omega t) + \frac{3}{4}A^2\omega k\frac{senh\,2k(k+z)}{senh^4(kh)}sen\,2(kx-\omega t) \tag{7}$$

where A is the wave amplitude (m), k is the wave number given by $k = 2\pi/\lambda$ (m^{-1}), d is the water depth (m), T is the wave period (s), ω is the frequency given by $\omega = 2\pi/T$ (rad/s), x is the streamwise coordinate (m), t is the time (s) and z is the normal coordinate (m).

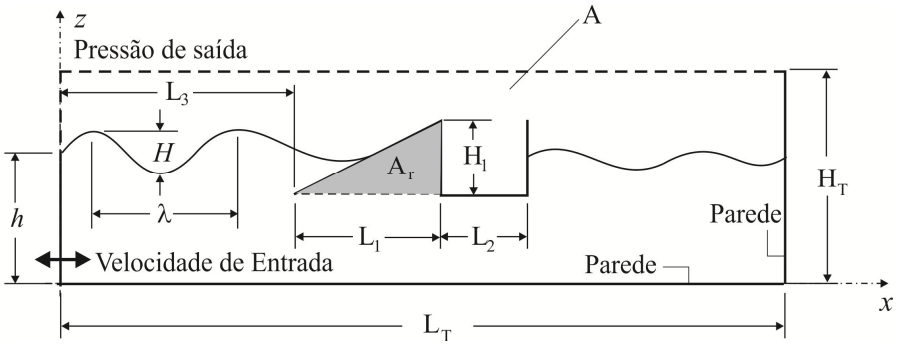

Figure 3. Sketch of the computational domain of the overtopping device inserted into the wave tank.

Concerning the other boundary conditions, the upper region of the left surface, as well as, the upper surface have prescribed atmospheric pressure (see the dashed surfaces in Fig. 3). In the other surfaces of the tank (lower and right surfaces) and in the overtopping surfaces the velocities are prescribed as null. For the initial conditions, it is considered that the fluid is still and the free water surface is $h = 0.6$ m.

For the numerical simulation of the conservation equations of mass and momentum, a commercial code based on the finite volume method (FVM) (FLUENT, 2007) is employed. The solver is pressure-based and all simulations were performed by upwind and PRESTO! for spatial discretizations of momentum and pressure, respectively. The velocity-pressure coupling is performed by the PISO method, while the GEO-RECONSTRUCTION method is employed to tackle with the volumetric fraction. Moreover, under-relaxation factors of 0.3 and 0.7 are imposed for the conservation equations of continuity and momentum, respectively. Concerning the spatial and temporal discretizations, it was employed a regular grid with triangular volumes of side $\Delta x = 0.01$ m and a time-step of $\Delta t = 1.00 \times 10^{-3}$ s.

4. RESULTS

Firstly, it is evaluated the influence of the ratio H_1/L_1 over the instantaneous mass flow rate for the transient flow, as can be seen in Fig. 4. It is observed step peaks for the cases $H_1/L_1 = 0.3$, 0.4, 0.9 and 1.0. However, the peaks are more prominent for the lower ratios than for the higher ones. Other observation is that for the lower ratios of $H_1/L_1 = 0.3$ and 0.4, the mass flow rate peaks occurred for $t = 8.1$ s and $t = 5.6$ s, respectively, while for the higher ratios of $H_1/L_1 = 0.9$ and 1.0, these peaks are only observed for $t = 13.5$ s and $t = 14.3$ s. In general, the transient behavior for the simulations with relative depth of $h/\lambda = 0.62$ are similar to the previous results for $h/\lambda = 0.5$ presented by Machado et al. (2011). It is also worthy to mention that the peaks obtained for $H_1/L_1 = 0.3$ and 0.4 are significantly higher than those obtained for the ratios $H_1/L_1 = 0.9$ and 1.0. For example, the highest peak obtained for the ratio $H_1/L_1 = 0.40$ ($\dot{m} = 3.80\, kg/s$) is nearly 452 % higher than the highest peak reached for $H_1/L_1 = 0.9$. Other important observation is that the peaks of instantaneous mass flow rate for $H_1/L_1 = 1.0$ is significantly suppressed for the relative depth of $h/\lambda = 0.62$ in comparison with the results obtained for $h/\lambda = 0.5$, which are presented in the work of Machado et al. (2011).

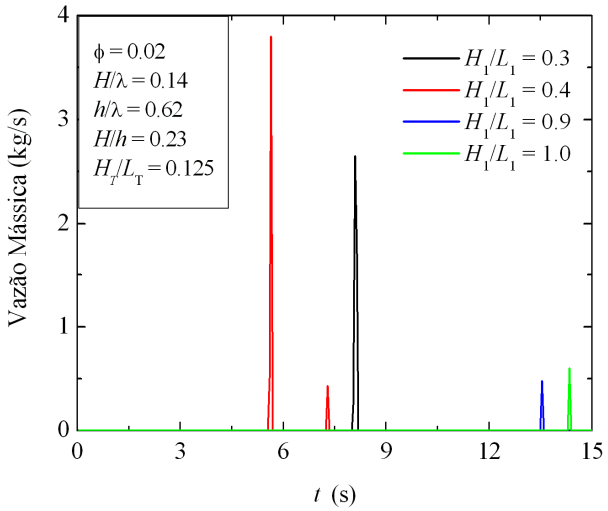

Figure 4. Instantaneous mass flow rate of water that insides the overtopping reservoir for the relative depth of $h/\lambda = 0.62$ for various ratios of H_1/L_1.

Figure 5 shows the effect of the ratio H_1/L_1 over the total amount of mass that enters into the reservoir along the time. In general, the behavior of the total mass as a function of H_1/L_1 was similar to that obtained in the previous study of Machado et al. (2011). For extreme ratios of H_1/L_1, both simulations ($h/\lambda = 0.50$ and 0.62) led to the worst results. However, the optimal shape was changed from $(H_1/L_1)_o = 0.6$ for $h/\lambda = 0.5$ to $(H_1/L_1)_o = 0.4$ for $h/\lambda = 0.62$. In this sense, there is no universal shape of overtopping ramp which leads to the best performance of device, i.e., for each wave climate the principle must be employed. The optimal shape $(H_1/L_1)_o = 0.4$ for $h/\lambda = 0.62$ conduct to an once maximized amount of mass that enters into the reservoir of $m_m = 0.24$ kg. Other important observation is concerned with a local point of maximum for $h/\lambda = 0.62$ at $H_1/L_1 = 1.0$, which was also noticed for the relative depth of $h/\lambda = 0.5$. However, the difference between the highest amount of mass and the local point of maximum is significantly more pronounced for $h/\lambda = 0.62$ (nearly 83 %) than for $h/\lambda = 0.5$ (nearly 16 %), i.e., the total mass which incomes the reservoir is strongly smoothed for the new wave condition studied in the present work.

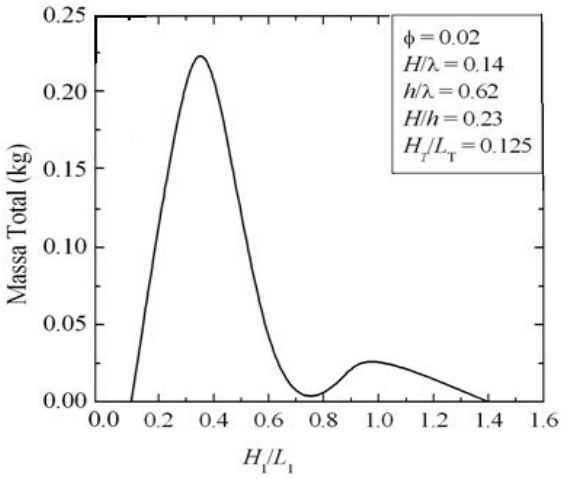

Figure 5. The effect of H_1/L_1 over the amount of mass that enters into reservoir for a wave climate with relative depth of $h/\lambda = 0.62$.

Figure 6 shows the wave behavior generated in the tank as a function of time for the lowest ratio of $H_1/L_1 = 0.10$. The topologies of volume fraction of water (blue) and air (red) are presented for the following instants of time: $t = 1.00$ s, 5.60 s, 7.30 s, 8.30 s and 9.65 s, Fig. 6 (a) – (e), respectively. In general, the behavior of topologies obtained here for $H_1/L_1 = 0.10$ is similar to that reached for the relative depth of $h/\lambda = 0.50$ (Machado et al., 2011), i.e., the non occurrence of overtopping is concerned with the high dissipation of kinetic energy imposed by the large length of the ramp. This dissipation is so intensive that is possible to notice the wave break, similar to observed in a beach.

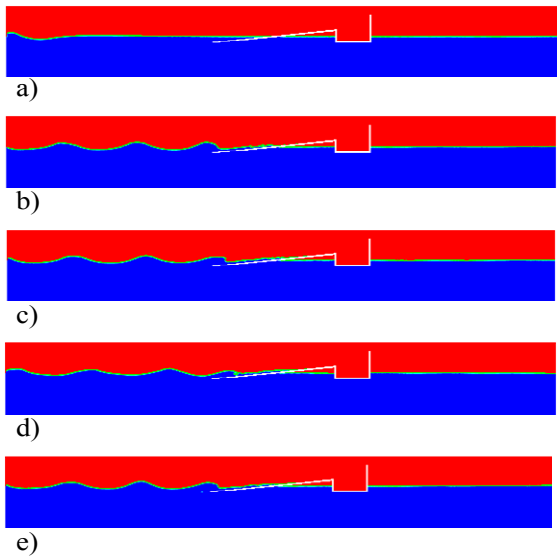

Figure 6. Transient behavior of wave flow ($h/\lambda = 0.62$) over the overtopping device for the ratio $H_1/L_1 = 0.10$ and for the following instants of time: a) $t = 1.00$ s; b) $t = 5.60$ s; c) $t = 7.30$ s; d) $t = 8.30$ s; e) $t = 9.65$ s.

Figure 7 shows the transient behavior for the wave generated in the tank for the highest ratio of $H_1/L_1 = 1.4$. The topologies for the flow are the same obtained in the previous case, i.e., $t = 1.00$ s, $t = 5.60$ s, $t = 7.30$ s, $t = 8.30$ s e $t = 9.65$ s (Fig. 7 (a) – 7 (e)). For this wave climate ($h/\lambda = 0.62$) the mechanism that avoids the overtopping is also the same observed for the relative depth of $h/\lambda = 0.5$. For this case, the ratio H_1/L_1 requires an elevate potential energy for occurrence of overtopping. However, for this ratio of H_1/L_1 the wave does not have this energy and the overtopping device becomes to act as a breakwater, smoothing significantly the wave energy, which can be clearly seems for the flow after the device (Fig. 7).

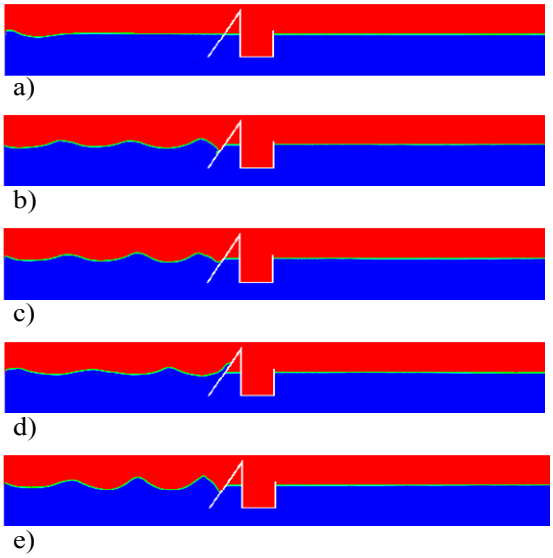

Figura 7. Transient behavior of wave flow ($h/\lambda = 0.62$) over the overtopping device for the ratio $H_1/L_1 = 1.4$ and for the following instants of time: a) $t = 1.00$ s; b) $t = 5.60$ s; c) $t = 7.30$ s; d) $t = 8.30$ s; e) $t = 9.65$ s.

Figure 8 shows the wave flow for the optimal ratio of $(H_1/L_1)_o = 0.40$. The topologies were also captured for the following instants of time: $t = 1.00$ s, $t = 5.60$ s, $t = 7.30$ s, $t = 8.30$ s e $t = 9.65$ s (Fig. 8 (a) – (e)). It can be noticed that for this case the wave reaches with a higher amount of energy than for extreme ratios of H_1/L_1, being this observation more evident for $t = 5.60$ s (Fig. 8(b)) and $t = 9.65$ s (Fig. 8(e)). This behavior is also noticed for the optimal shape $(H_1/L_1)_o = 0.6$ at a relative depth of $h/\lambda = 0.5$. It is worthy to mention that, for the wave climate evaluated here, the wave reaches the overtopping device with a lower amount of energy in comparison with the simulation of $h/\lambda = 0.5$. This fact influences the mass flow rate that enters into the reservoir leading to a decrease of the optimal ratio from $(H_1/L_1)_o = 0.6$ for $h/\lambda = 0.5$ to $(H_1/L_1)_o = 0.4$ for $h/\lambda = 0.62$.

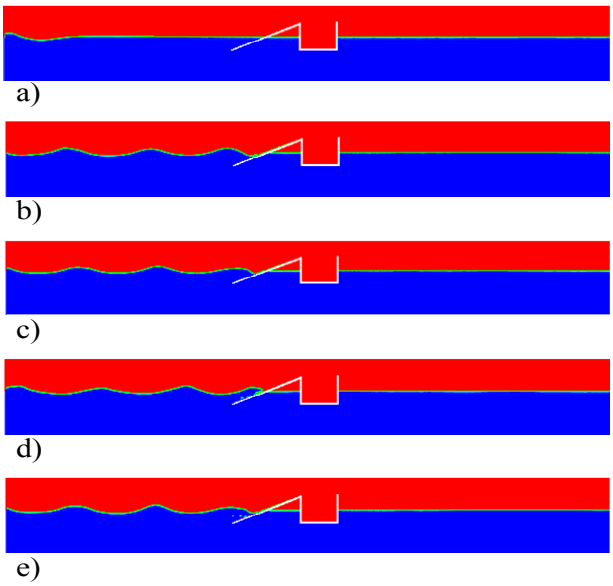

Figura 8. Transient behavior of wave flow ($h/\lambda = 0.62$) over the overtopping device for the ratio $H_1/L_1 = 0.4$ and for the following instants of time: a) $t = 1.00$ s; b) $t = 5.60$ s; c) $t = 7.30$ s; d) $t = 8.30$ s; e) $t = 9.65$ s.

5. CONCLUSIONS

In the present work it is being performed a numerical study seeking the best geometries (a theoretical recommendation) for the shape of the main operational principle of an overtopping device for a relative depth of $h/\lambda = 0.62$. For the laminar, two-dimensional, transient flow of the mixture water-air it is solved numerically the conservation equations of mass, momentum and one additional equation for the volume fraction transport. The method Volume of Fluid (VOF) was used to tackle with the mixture water-air. The results showed that the lowest and highest ratios of H_1/L_1 led to the worst performance of the system, similarly to the previous observations of Machado et al. (2011) for the

simulations with the relative depth of $h/\lambda = 0.5$. It was also observed that the local point of maximum obtained for $H_1/L_1 = 1.0$ was significantly suppressed for the present case in comparison with the case with $h/\lambda = 0.5$. For example, differences between the total mass that enters into reservoir for the optimal shape and the local point of maximum was approximately 86 % for $h/\lambda = 0.5$ and 16 % only for $h/\lambda = 0.62$.

The most important conclusion of this study is concerned with the optimal shape for design of overtopping devices. Constructal Design for WECs showed that there is no universal shape that leads to the best performance of device for several wave climates. For the present study for $h/\lambda = 0.62$, the optimal shape was reached for $(H_1/L_1)_o = 0.4$ while for other relative depth ($h/\lambda = 0.5$) the simulations showed that the optimal shape is reached for $(H_1/L_1)_o = 0.6$.

6. ACKNOWLEDGEMENTS

The authors thank CNPq for the financial support (Process: 555695/2010-7). L. A. O. Rocha, P. R. F. Teixeira and J. A. Souza also thank CNPq for research grant. E. D. dos Santos thanks FAPERGS by financial support.

7. REFERENCES

Beels, C., Troch, P., De Visch, K., Kofoed, J. P., De Backer, G., 2010, Application of the time-dependent mild-slope equations for the simulation of wake effects in the lee of a farm of Wave Dragon wave energy converters, Renewable Energy, Vol. 35, pp. 1644 – 1661.

Bejan, A., Lorente, S., Theory of generation of configuration in nature and engineering, J. Appl. Phys.100 (2006).

Bejan, A., Lorente, S., 2008, Design with Constructal Theory, John Wiley and Sons Inc.

CENTER FOR RENEWABLE ENERGY SOURCES, Wave Energy Utilization in Europe**.** Disponível em: <http://wave-energy.net/Library/WaveEnergy_Brochure.pdf>, 2002.

Cruz, J.; Sarmento, A. Energia das Ondas – Introdução aos Aspectos Tecnológicos, Econômicos e Ambientais. Instituto do Ambiente, 2004.

Didier, E.; Neves, M.G. A Lagrangian Smoothed Particle Hydrodynamics – SPH – Method For Modelling Waves-Coastal Structure Interaction. In proceedings of the European Conference on Computational Fluid Dynamics, Portugal, 2010.

Falcão, A. F. O., 2010, Wave energy utilization: A review of the technologies, Renewable and Sustainable Energy Reviews, Vol. 14, pp. 899 – 918.

FLUENT (version 6.3.16), ANSYS, Inc., 2006.

Gomes, M. N.; Isoldi, L. A.; Olinto, C. R. Rocha, L. A. O.; Souza, J. A. Simulação numérica e otimização do comprimento de um dispositivo do tipo coluna d'água oscilante. Congresso Ibero-Latino-Americano de Métodos Computacionais em Engenharia (CILAMCE), Brasil, 2009.

Iahnke, S. L. P. Estado da Arte e Desenvolvimento de um Modelo de Simulação Numérica para o Princípio de Galgamento, 2010. Dissertação (Mestrado em Modelagem Computacional) – Curso de Pós Graduação em Modelagem Computacional, Universidade Federal do Rio Grande.

Lima, J. A. O. Gerador de Baixa Rotação para Aproveitamento de Energia das Ondas, Dissertação de Mestrado. Universidade Nova de Lisboa, Portugal, 2010.

Liu, Z., Hyun B., Hong, K. Aplication of Numerical Wave Tank to OWC air chamber for wave energy conversion. International Offshore and Polar Engineering Conference, Canada, 2008a.

Liu, Z., Hyun B., Jin, J. Numerical Prediction for Overtopping Performance of OWEC, Journal of the Korean Society for Marine Environmental Engineering, Vol. 11, No.1, 2008b.

Machado, B. N.; Zanella, M. M.; Gomes, M. N.; Teixeira, P. R. F.; Isoldi, L. A.; Dos Santos, E. D.; Rocha, L. A. O.; 2011. Constructal Design of an Overtopping Wave Energy Converter, Proceedings of Constructal Law Conference, Porto Alegre, Brazil.

Neves, M.G.; Reis, M.T.; DIDIER, E. Comparison of wave overtopping at coastal structures calculated with Amazon, Cobras-UC and SPHysics. V European Conference on Computational Fluid Dynamics, Portugal, 2010.

Relatório do WAVEC. Potencial e Estratégia de Desenvolvimento da Energia das Ondas em Portugal. Wave Energy Centre, 2004.

Ribeiro, I. B., Metodologia para Escolha de uma Tecnologia de Conversão de Energia das Ondas. Projeto de Graduação. Universidade Federal do Rio Grande, Rio Grande – RS, 2007.

Tedd, J. Kofoed, J. P. Measurements of overtopping flow time series on the Wave Dragon, wave energy converter, Renewable Energy, Vol. 34, 2009.

Tolmasquim, M. Fontes Renováveis de Energia no Brasil. Rio de Janeiro: Interciência: CENERGIA, 2003.